IEEE Robotics and Automation Letters (RAL) paper presented at the
2020 IEEE/RSJ International Conference on Intelligent Robots and Systems (IROS)
October 25-29, 2020, Las Vegas, NV, USA (Virtual)

Modular, Accessible, Sensorized Objects for Evaluating the Grasping and Manipulation Capabilities of Grippers and Hands

Geng Gao[1], Gal Gorjup[1], Ruobing Yu[2], Patrick Jarvis[2], and Minas Liarokapis[1]

***Abstract*— The human hand is Nature's most versatile and dexterous end-effector and it has been a source of inspiration for roboticists for over 50 years. Recently, significant industrial and research effort has been put into the development of dexterous robot hands and grippers. Such end-effectors offer robust grasping and dexterous, in-hand manipulation capabilities that increase the efficiency, precision, and adaptability of the overall robotic platform. This work focuses on the development of modular, sensorized objects that can facilitate benchmarking of the dexterity and performance of hands and grippers. The proposed objects aim to offer; a minimal, sufficiently diverse solution, efficient pose tracking, and accessibility. The object manufacturing instructions, 3D models, and assembly information are made publicly available through the creation of a corresponding repository.**

I. Introduction

With the ever increasing presence of robotic agents in factory and home environments, significant industrial and research effort has been put into the development of dexterous robot hands and grippers. Such end-effectors offer robust grasping and dexterous, in-hand manipulation capabilities that increase the efficiency, precision, and adaptability of the system to different task requirements. Even though equivalent dexterity from an object-centric viewpoint could possibly be achieved by a dexterous robot arm paired with a simple gripper, a dexterous end-effector is often more appropriate [1]. Good examples are tasks that require in-hand tool re-orientation (without re-grasping) or tasks in cluttered environments where arm motion is heavily constrained.

Currently, many dexterous end-effector variants are available to a robot system designer, ranging from anthropomorphic hands [2]–[4], to more task-oriented grippers [5], [6]. Even though each design is generally accompanied by a range of tests and experiments highlighting selected performance aspects, it remains challenging to assess which hand is most appropriate for a specific application. This is particularly relevant for tasks that require a certain degree of in-hand manipulation capability, where a unified performance evaluation standard is yet to be adopted. Defining meaningful benchmarking methods for in-hand manipulation is difficult because the protocols are closely linked to the objects used in the tests. Manipulation tasks generally involve complex physical phenomena that can not be appropriately evaluated in a simulated environment, so challenging and time-consuming real experiments are required to obtain reliable results.

Fig. 1. The proposed sensorized object set consists of primitive shapes in three sizes that can be reassembled in various combinations. The surface friction and stiffness can be selected by employing different molding materials. Object halves contain cavities enabling the adjustment of weight and weight distribution in objects. The object set has been designed to be compatible with a variety of motion capture sensing options such as the magnetic motion capture micro-sensors of the Polhemus Liberty, retroreflective markers for tracking with an optical motion capture system (e.g., Vicon), ArUco markers that can be tracked with a camera, or an inertial measurement unit (IMU).

When defining a benchmark it is important to choose an appropriate object set that has the following characteristics:

1) **Allow for Efficient Pose Tracking:** Unlike grasping, in-hand manipulation performance can rarely rely on discrete success metrics, so precise object motion tracking is of paramount importance for the creation of useful benchmarks. The object set should therefore be able to accommodate some form of motion capture technology, which is absent in most existing sets.
2) **Provide a Minimal, Sufficiently Diverse Solution:** The object set needs to be diverse enough to cover the broad range of applications and compact enough to permit fast and effortless testing and experimentation. A minimal set will also allow for easy storage.
3) **Provide Accessibility:** A condition for widespread adoption of unified benchmarking frameworks is that the object set used should be easily accessible to users and research groups anywhere in the world.

This work was supported by Humanoid Artificial Intelligence under Auckland UniServices Limited grant agreement #5000550.

[1]Geng Gao, Gal Gorjup, and Minas Liarokapis are with the New Dexterity research group, Department of Mechanical Engineering, The University of Auckland, New Zealand. E-mails: {ggao102, ggor290}@aucklanduni.ac.nz, minas.liarokapis@auckland.ac.nz

[2]Ruobing Yu and Patrick Jarvis are with the Humanoid Artificial Intelligence, USA. E-mails: ruobing@humanoidartificialintelligence.com, patrickj@aidatainnovations.com

This work presents a modular, sensorized object set for assessing the grasping and dexterous, in-hand manipulation capabilities of grippers and hands. To facilitate object motion tracking, the set is equipped with modules that can accommodate various motion capture markers or sensors. These removable sensor mounts are designed to have a negligible effect on the objects' inertia and to minimally obstruct their motion. The size vs diversity trade-off is solved through a modular design, allowing the user to mix and match object parts and obtain a large selection of different shapes from a small number of initial components (minimal set). The objects contain cavities that can be utilized to adjust their weight and its distribution, if required. The objects come in rigid and soft surface variants, allowing the user to assess performance with different contact conditions. The set solves the accessibility issue by employing common rapid prototyping methods in its fabrication process and making use of easily accessible materials. The object design and manufacturing instructions are made available in an open source manner.

Even though the main application of the proposed object set is gripper and hand performance assessment, it is also suitable for a wide range of alternative use cases. Beyond providing quantitative measures for hand capability and dexterity comparisons, the objects can be of great use in human arm or hand rehabilitation and clinical assessment. The patient's level of recovery can be effectively monitored and used as a basis for designing case-specific training sessions that focus on weakened muscle groups. As the objects are compatible with several types of motion capture systems, they allow for efficient comparison of tracking performance.

The rest of this work is organized as follows: Section II introduces the related work, Section III presents the design of the objects, Sections IV demonstrates how the proposed objects can be used, while Section V concludes the work and discusses some possible future directions.

II. Related work

For dexterous robotic hands, the majority of object set resources focuses on grasping and manipulation that largely depend on robot arm dexterity. Although some of the previously proposed objects are equipped with motion tracking capabilities and tactile sensors, there are no examples of easily accessible, modular, sensorized solutions. Moreover, most of the object sets proposed are mainly used to evaluate the grasping capabilities of both grippers and hands and not their efficiency in executing dexterous manipulation tasks.

Even though object sets are necessary for reliable evaluation of a robot's manipulation performance in the real world, only a few are clearly defined and available to the research community. The YCB object set [7] is a set of 75 objects and their corresponding 2D image and 3D model data. The set is aimed at benchmarking the capabilities of robot end-effectors for a wide range of tasks and consists of everyday life objects, objects used in assembly tasks during medical rehabilitation, and objects for industrial robotic applications. It is currently the most well known and complete object set available that focuses mainly on quantifying a robot arm-hand system's ability to grasp and manipulate objects. The set can also be augmented with visual markers for in-hand manipulation [8], although this is not the collection's primary purpose. The YCB object set is readily available upon request. Another list of physical objects was presented within the frame of the Amazon Picking Challenge [9], where the picking task was perception oriented and object models were not provided. Building on the former, the ACRV Picking Benchmark [10] defines a set of 42 common objects and their labeled images for an extended shelf picking benchmark.

Although they are not part of a standard set, some instances of individual sensorized objects for assessing grasping and manipulation capabilities of human and robot hands have been developed. In [11], two instrumented objects for investigating human grasp properties were presented. The objects were designed to assess only three-finger grasp configurations, focusing on contact force measurements. In [12], the authors presented an object equipped with tactile and motion tracking sensors, which was in [13] utilized to evaluate human grasp quality. These are not readily available to the research community and their manufacturing procedures are not trivial, making widespread adoption difficult.

An object collection that was not explicitly defined, but is perhaps the closest to this proposal, was employed within a standard defined by NIST [14], which was further explored in [15]. The standard presents the foundations for robot hand performance benchmarking and among others includes protocols for quantifying in-hand manipulation and object pose estimation. Although the benchmark recognises the importance of object shapes and properties on dexterous manipulation performance, it does not define a standard set to be used in the experiments. It does, however, advise that the tests should be conducted across a range of diverse objects. Their examples include a cube, sphere, and cylinder that have been retrofitted with reflective markers for tracking with a visual motion capture system. The external marker mount is quite large compared to the objects, affecting their inertial properties and possibly hindering the execution of certain in-hand manipulation motions. To address those issues, the objects proposed in this work are equipped with motion capture sensors in a way that preserves the object shape and inertia characteristics.

A number of data sets that consist of object scans, images, and models have also been proposed. These are appropriate for experiments and planning in simulation, or as training sets for various machine learning algorithms. BigBIRD [16], for instance, features a data set providing high quality image and 3D point cloud data for each of its 125 objects. Another example is the KIT object models database [17], which is targeted at applications in service robotics. It consists of 3D point cloud data, aligned with 2D images for over a hundred typical household items. A large scale endeavor aimed mainly at grasp planning is the Columbia Grasp Database [18], which provides 3D models of roughly 8000 objects, along with successful grasp labels for many robot hands.

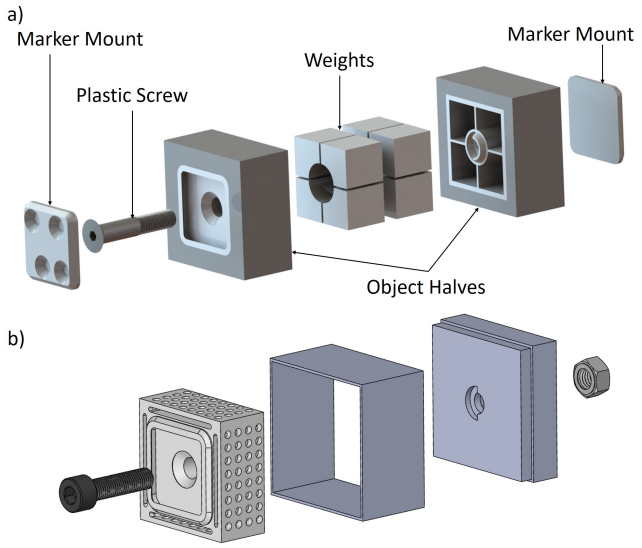

Fig. 2. The proposed construction of the modular, sensorized soft cube is depicted in subfigure a). Starting from the left of the figure, the sensorized object consists of a urethane based retroreflective marker mount, a plastic screw, one object half, the object weights, the other object half, and another urethane based retroreflective marker mount. The urethane mount houses four retroreflective marker sockets that are configured asymmetrically, to allow reliable 6 DOF (degrees of freedom) pose tracking with an optical motion capture system (e.g., Vicon). To minimise occlusion issues, the mounts are placed on opposing object faces. Subfigure b) shows the exploded view of a mold for a soft cube.

III. Modular, Sensorized Objects

In this work, a range of modular, sensorized objects is created by combining a set of primitive object shapes. The structures of the sensorized objects consist of five to thirteen modular, 3D printed parts. In particular, the list is as follows: a plastic screw (which holds the object parts together), two object halves, two removable urethane marker mounts, and eight removable object weights (these are optional components). Such a structure is depicted in Fig. 2, subfigure a). The proposed objects can be created with a variety of materials that facilitate the selection of the desired object stiffness and friction and they can be equipped with different motion tracking markers and sensors.

A. Object Geometries

The object set consists of sphere, cube, and cylinder object halves (the cylinder is split both axially and radially), which can be joined together to form a combination of diverse objects for grasping and manipulation experiments (see Fig. 3). The different shape combinations are based on a minimal number of parts that achieves a diverse set of simple and complex geometries. Geometries with sharp bends or corners (the objects of Fig. 3d) force end-effectors to perform more complex manipulation motions like finger gaiting [19] or to maneuver around the object geometry in order to reach certain object surfaces. Such complex motions give to the researchers insight into how certain hands or grippers will behave when handling geometrically complex objects. Additionally, three object sizes have been developed to be used with a wide range of hand and gripper sizes. The three sizes for cylindrical objects can be seen in Fig. 3e and all object dimensions can be found in Table I.

TABLE I

The dimensions of the proposed sensorized objects for different object sizes and geometries.

Object Geometry		Dimensions [mm]
Small	Cube	50 x 50 x 50
	Cylinder (Radially Split)	50 x 50
	Cylinder (Axially Split)	50 x 50
	Sphere	50
Medium	Cube	75 x 75 x 75
	Cylinder (Radially Split)	75 x 75
	Cylinder (Axially Split)	75 x 75
	Sphere	75
Large	Cube	100 x 100 x 100
	Cylinder (Radially Split)	100 x 100
	Cylinder (Axially Split)	100 x 100
	Sphere	100

B. Material Selection

Each object half contains four compartments, which can be filled or left empty to generate various controllable weights and variations of center of mass in an object. The introduction of an easily tunable center of mass in the proposed objects allows for rapid adjustment of the experimental conditions while assessing the robustness and dexterity of a hand, by altering a single object characteristic.

The achievable mass variations depend on the density of the selected material. The maximum achievable weight deviations of the proposed sensorized objects for different materials can be found in Table II. It must be noted that when using a magnetic motion capture system, metallic weights must be avoided. Surface friction and hardness can be varied in different object halves by combining different elastomer materials molded onto the rigid part. Elastomer materials with Shore hardness of 30A (Youngs Modulus of 1.07 MPa) and above (like urethane rubbers, e.g. Smooth-On Vytaflex 30) are all compatible materials for producing various surface frictions and stiffnesses.

C. Fabrication / Assembly Process

To increase accessibility, rapid prototyping methods like hybrid deposition manufacturing (HDM) [20] and 3D printing were utilized. These techniques employ a simple fabrication process and allow for efficient integration of various materials (e.g., polylactic acid (PLA), Acrylonitrile butadiene styrene (ABS), resin, etc.). The object set can thus be made in a short time frame while remaining affordable.

TABLE II

MAXIMUM ACHIEVABLE WEIGHT DEVIATIONS OF THE PROPOSED SENSORIZED OBJECTS. ALL OBJECTS ARE CONSIDERED TO BE SOLID (NON-HOLLOW). DIFFERENT MATERIALS CAN BE CHOSEN FOR THE FABRICATION OF THE OBJECT SET.

Object Geometry		**Max Internal Weight Deviation [g]**				
		PLA	ABS	PETG	Resins	Aluminium
Small	Cube	42.56	35.70	47.36	39.47 - 42.90	92.66
	Cylinder (Radially Split)	27.97	23.46	31.13	25.94 - 28.20	60.91
	Cylinder (Axially Split)	29.07	24.38	32.35	26.96 - 29.30	63.29
	Sphere	17.26	14.48	19.21	16.01 - 17.4	37.58
Medium	Cube	248.20	208.17	276.22	230.18 - 250.20	540.43
	Cylinder (Radially Split)	167.65	140.61	186.58	155.48 - 169.00	365.04
	Cylinder (Axially Split)	183.12	153.59	203.80	169.83 - 184.60	398.74
	Sphere	148.40	124.47	165.16	137.63 - 149.60	323.14
Large	Cube	731.40	613.43	813.98	678.32 - 737.3	1592.57
	Cylinder (Radially Split)	517.72	434.22	576.18	480.15 - 521.90	1127.30
	Cylinder (Axially Split)	544.21	456.44	605.65	504.71 - 548.60	1184.98
	Sphere	422.79	354.60	470.52	392.10 - 426.20	920.59

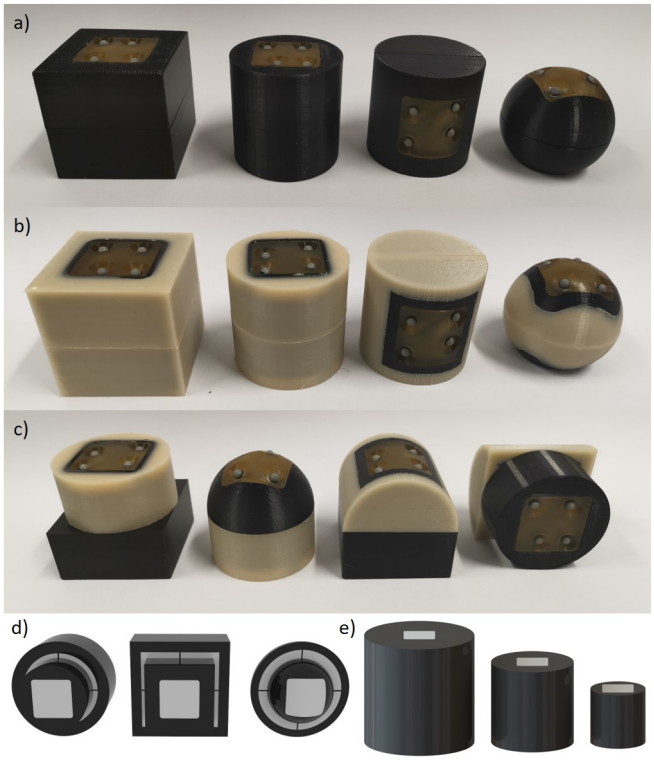

Fig. 3. Subfigures a) and b) present the primitive shapes of proposed rigid and soft sensorized object variants, respectively. Subfigure c) demonstrates examples of irregularly shaped configurations obtained by combining the modules. Subfigure d) shows a set of objects with varying sizes that can be used with hands of different sizes.

1) 3D Printing Components: The rigid bodies and molding components of the proposed sensorized objects are produced through 3D printing. Object halves with rigid outer surfaces (PLA or ABS material) are printed directly and do not require additional molding steps. Object halves with compliant, elastomer surfaces and alternative friction properties require 3D printing of various molds and inner object cores that facilitate molding. The inner object cores are designed as object halves with a porous outer wall that interlocks and anchors the elastomer material in place.

2) Mold Assembly: Depending of the module being fabricated, the mold assembly steps can vary from preparation of a single mold part, to the assembly of several mold components around a soft object core (as it can be seen in Fig. 4a) for the material deposition step.

3) Deposition: Once a mold is assembled, the selected elastomer material is deposited into the mold cavity, as depicted in Fig. 4b. The elastomer can be used to produce appropriate mounts for attaching retroreflective markers or ArUco markers, or to cover the object halves, providing varying object surface properties.

4) Mold Disassembly: After the curing process is completed, the molded components can be removed from the molds and assembled together with the other 3D printed parts to produce a complete object, as shown in Fig. 4d.

The CAD and STL files of the sensorized objects, as well as detailed fabrication and assembly instructions, can be found at the following URL:

https://github.com/newdexterity/Sensorized-Objects

TABLE III

COMPARISON OF DIFFERENT MOTION CAPTURE SYSTEMS.

Motion Capture System	**Accuracy**		**Noise**		**Sampling Rate** [Hz]
	Translation [mm]	**Rotation** [deg]	**Translation** [mm]	**Rotation** [deg]	
Optical Motion Capture	0.076 - 0.129	0.48 - 0.82	0.015	0.095	100
Magnetic Motion Capture	0.76	0.15	0.017	0.05	240
ArUco Markers	1.90 - 2.17	0.59 - 1.12	0.77 - 5.57	0.076 - 0.26	30
IMU	N/A	1.25	N/A	0.055	104

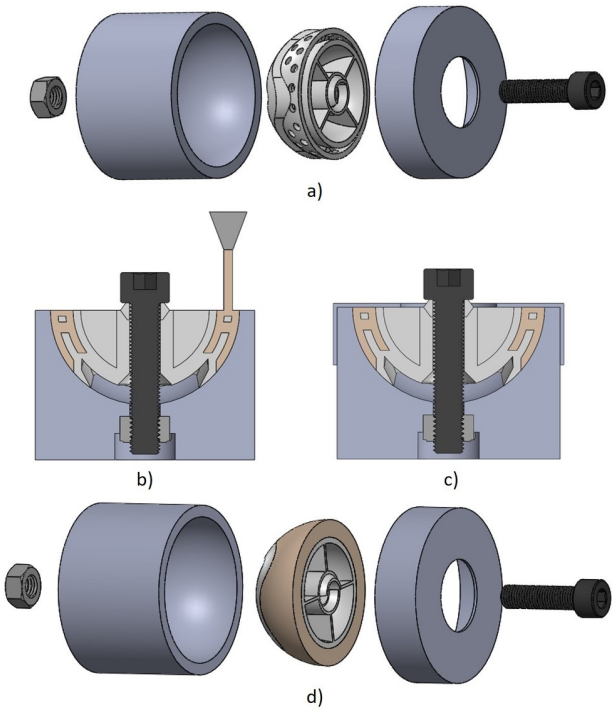

Fig. 4. Molding process for creating a soft-surface sphere half. Subfigure a) displays the assembly of molding components for a soft sphere half. Subfigures b) and c) present the deposition process, where elastomer material is injected into the cavity of the mold and then sealed to achieve the required outer surface. Subfigure d) shows the disassembly after the elastomer material has been cured.

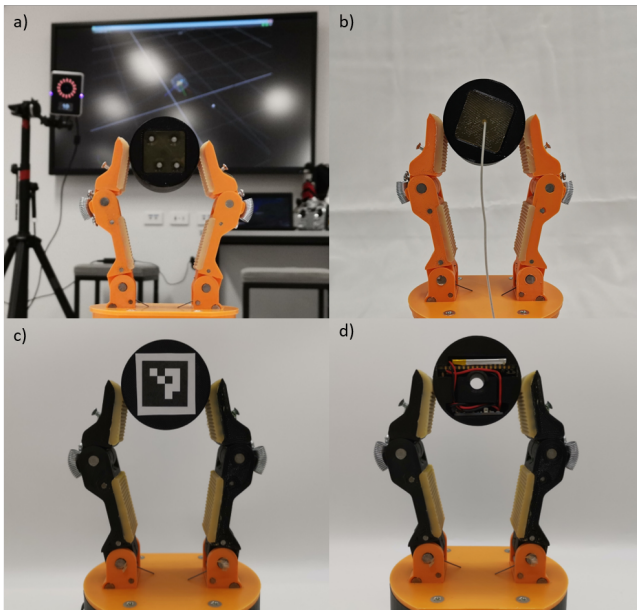

Fig. 5. Instances of an experiment conducted with a sensorized object and a simple, two fingered gripper executing an equilibrium point manipulation task. The object motion tracking is accomplished with: a) the Vicon optical motion tracking system that utilizes reflective markers, b) the Polhemus Liberty magnetic motion capture system that employs a micro sensor inserted in the object core through the urethane pad, c) the ArUco marker attached to a urethane pad tracked through a standard web camera, and d) the IMU attached inside an object half.

D. Sensing

The object set was made compatible with four motion capture system types that allow accurate trajectory tracking. The first is an optical motion capture system (e.g., Vicon), which utilizes retroreflective markers for tracking the object pose, as seen in Fig. 5a. The second is a magnetic motion capture system (e.g., Polhemus Liberty), the micro sensor of which can be mounted inside a properly designed plastic screw (Fig. 5b), reaching the center of the object. The third is based on an inertial measurement unit (IMU), along with a microcontroller and bluetooth module (Ardunio NANO 33 IoT), powered by a 180 mAh lithium polymer battery. These components are fixed within the object half with dedicated cavities, as depicted in Fig. 5d. The IMU system is accompanied by sample Arduino code that performs orientation tracking using the Madgwick filter [21] and publishes the angles through Bluetooth. Position tracking with the IMU system was not implemented due to the high sensitivity to acceleration error in the double integration process. In case none of the first three systems is available to the users, a set of marker mounts compatible with Augmented Reality (AR) tags or ArUco markers is provided (Fig. 5c).

A comparison of the supported motion capture systems characteristics is presented in Table III. The translation accuracy and noise (precision) for the optical motion capture system (Vicon) were obtained from [22]. The rotation accuracy and noise values for the Vicon system were estimated with respect to the retroreflective marker separation on the sensor pad. The accuracy values for the magnetic motion capture systems were obtained from the Polhemus Liberty user manual [23]. The noise values for the magnetic motion capture system were obtained from static sensor measurements. The accuracy and noise characteristics for AR tag based motion tracking were obtained experimentally, using the ArUco class of fiducial markers [24] and a Logitech C922 Pro Stream HD webcam with 1080p resolution at 30 frames per second. A marker of size 25 mm was attached to a sensorized cube and tracked with the webcam. The cube was simultaneously tracked with the Vicon system, which was chosen as the ground truth. For this purpose, larger Vicon markers were placed with higher separation along the object to ensure higher tracking accuracy. The translational accuracy was estimated by linearly offsetting the cube and comparing the distances measured by the two systems. The rotational accuracy was estimated by rotating the cube by 90 degrees along a fixed axis and comparing the measured angles. The translational and rotational noise was computed as the standard deviation of the position and angle offsets from the mean estimated pose in a static configuration. The accuracy and noise experiments for the ArUco markers were performed at 20 cm and 100 cm from the camera. The rotation accuracy and noise for the IMU system were obtained in a similar fashion, using the Vicon system as reference.

Depending on the manipulation task, the best suited motion capture system could change. For instance, the optical motion capture system (Vicon) offers data with the highest accuracy and a low amount of noise. However, when conducting more complex manipulation motions such as caging manipulation, the markers may be covered by the hand, causing occlusions and affecting the data collection process. This effect can also be observed in the AR tags and ArUco markers, where the tags and markers must be visible to the camera. The magnetic motion capture system (Polhemus Liberty) mitigates the occlusion issue of the previous two systems, but is sensitive to the presence of large metallic objects. The thin micro-sensor cable of the magnetic motion capture system may impact the object dynamics if there is tension on the cable, and may obstruct the hand's motion when performing certain manipulation tasks. The IMU system does not suffer from occlusion issues and can operate untethered, but it can not be accommodated by all object sizes (e.g., the small rigid sphere, and the small soft objects range) due to size limitations of the employed electronics (i.e., microcontroller board, battery, and step-up regulator). Another disadvantage of the IMU system is the significant drift that affects position tracking. The distinct disadvantages of the four examined motion capture systems can be mitigated by taking advantage of the multi-modal sensing capabilities of the proposed sensorized object set. By combining different classes of motion capture approaches, the quality and accuracy of the captured data can be significantly improved. For instance, a low-cost solution for full object pose tracking can rely on AR tags and the IMU, fusing the two data streams to compensate for occlusion and drift issues of the separate systems. The proposed object set does not incorporate force sensing modules to preserve fabrication simplicity, object size, and overall accessibility. Furthermore, the lack of such additional sensors allows the set to be highly reconfigurable and maintain a low cost. Even though measuring force values and profiles is essential for many manipulation tasks, there are several aspects of dexterous, in-hand manipulation that can be effectively assessed purely through object pose tracking and object kinematics. For such applications, the proposed object set is very well suited.

E. Object Models

The objects were designed in the SolidWorks CAD software, and the resulting source models were made available through the accompanying sensorized objects website and repository. Disseminating source designs allows for fast parameter modification and extraction, facilitating community involvement in improving and evolving the object set. The repository also contains STL models of all objects, which can be readily used with various rapid prototyping methods. In addition, the models can be used as collision objects in various planning frameworks, as well as for point cloud registration in perception systems. Combined with the provided mass and surface material data, the object models can also be effectively utilised in simulated environments. They are very well suited for simulation-to-reality applications, as their integrated tracking capability enables straightforward comparison between simulated and real trajectories.

IV. Functional Demonstration

The pose tracking capability of the sensorized objects can be used to give insight into the ranges of motion, repeatability, and drift of the system. It can be employed to assess and compare the performance of robot hands and grippers, as well as human hands, as depicted in Fig. 6. The objects can also provide pose feedback to the hand to quickly test closed-loop control algorithms. Through the highly accessible and customizable shapes and weights of objects that the proposed set offers, the time needed to prepare experimental examples can be significantly reduced.

For demonstration purposes, a performance assessment of the NDX-A* hand [25] was conducted, as presented in Fig. 7. The demonstration examines the robot hand's robustness in executing a combined rolling and translation manipulation motion over 10 cycles with a chosen sensorized object. The hand's performance was assessed in terms of drift and repeatability for the executed manipulation motion, computed from the cycle endpoints. Drift was computed by averaging the positional and rotational differences between subsequent endpoints. Repeatability was calculated as the

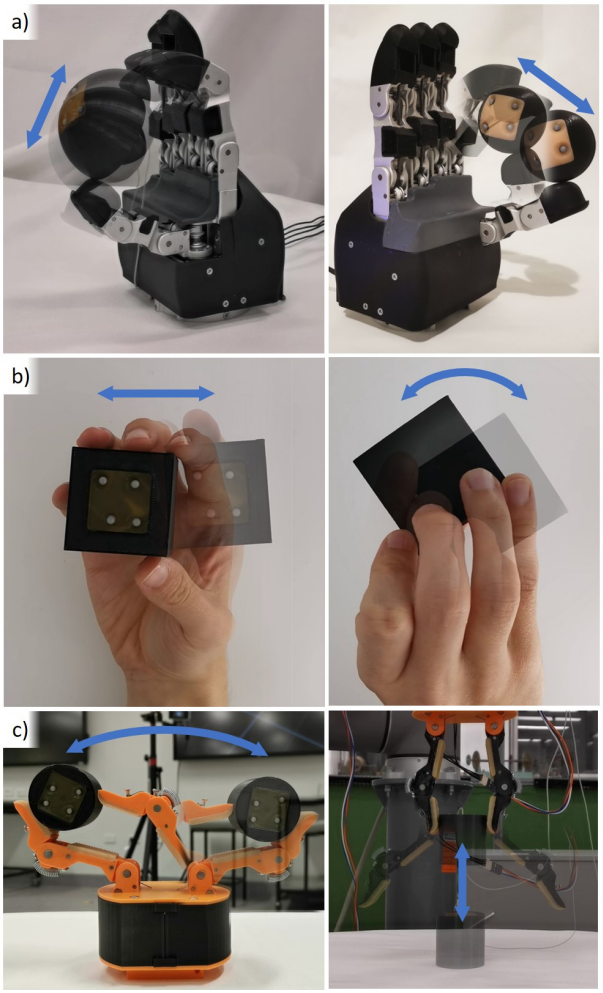

Fig. 6. The functional demonstration shows various objects from the sensorized object set being manipulated with different in-hand manipulation strategies by different hands and grippers. Subfigure a) displays an NDX-A* robot hand [25] performing fixed point and rolling manipulation motions. Similarly, subfigure b) shows in-hand translation and rotation tasks executed by the human hand. The T42 gripper [26] is used to perform manipulation, as well as grasping and releasing experiments in subfigure c).

average positional and rotational difference between the initial end point and the drift-corrected cycle endpoints. The experiments were performed with a small rigid-surface sphere and a soft-surface sphere without additional weights, tracked with the Polhemus Liberty motion capture system. Although the robot hand is composed of metallic components, the noise can be significantly minimized by ensuring the magnetic sensor is close to the Polhemus source and by avoiding grasps that enclose the sensor in metal, such as caging grasps. The results (Table IV and Fig. 7) can give insight into whether a certain end-effector is suitable for a chosen task based on the maximum acceptable error for that task. Furthermore, they can be used for diagnosing slip in the system through controlled variation of individual object and motion characteristics, in this case the surface compliance. For instance, the obtained drift results indicate a need for increased finger pad friction or increased contact forces that should be exerted on the object.

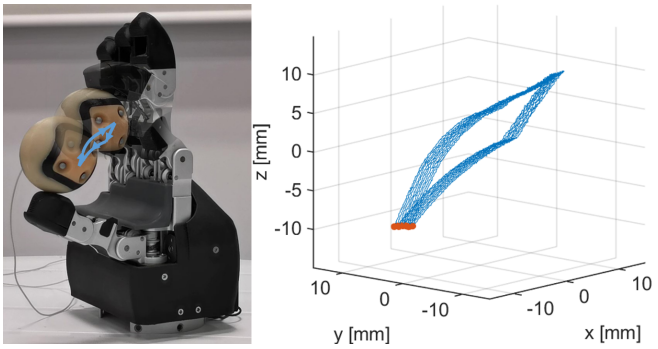

Fig. 7. Experimental data of a manipulation task executed with a soft sphere and the NDX-A* robot hand. Ten trials of the manipulation task have been executed. Cycle end points (highlighted in red) enable a holistic assessment of the repeatability and drift. Such data also allows the user to assess the performance and dexterity of the employed gripper or hand.

TABLE IV

MANIPULATION REPEATABILITY AND DRIFT FOR TWO DIFFERENT OBJECT SURFACES FOR A SPHERICAL OBJECT.

Manipulation Results		**Rigid Surface**		**Soft Surface**	
		Mean	**Standard Deviation**	**Mean**	**Standard Deviation**
Repeatability	Translation [mm]	0.26	0.18	0.21	0.12
	Rotation [deg]	1.27	0.59	0.4	0.14
Drift	Translation [mm]	0.33	0.14	0.22	0.11
	Rotation [deg]	2.35	0.01	0.87	0.002

A webpage presenting the object set and a video with experiments can be found at the following URL:

http://newdexterity.org/sensorizedobjects

V. CONCLUSIONS AND FUTURE DIRECTIONS

This work focused on a modular and accessible sensorized object set for benchmarking the grasping and dexterous, in-hand manipulation capabilities of human and robot hands. The object models, fabrication processes, and assembly information have been discussed and have been made publicly available. A series of experiments involving the proposed sensorized objects have been conducted and paradigmatic experimental data has been presented. Regarding future directions, the object set can be extended to include additional shapes and softer surface materials. As the set is modular, this would exponentially increase the number of possible configurations and testing conditions. The object collection can also be adapted to allow assessing tasks closer to real-life applications, such as screwing, pouring, and insertion. Implementation of a set of accompanying benchmarks and protocols can enhance the utilization of the object set and

give researchers additional ways in which the objects can be used. Another possible direction would be to add force sensing capabilities to the proposed objects.

ACKNOWLEDGEMENT

The authors would like to thank Che-Ming Chang and Anany Dwivedi for their valuable insight and feedback during the writing and internal review of this paper.

REFERENCES

[1] I. M. Bullock, R. R. Ma, and A. M. Dollar, "A hand-centric classification of human and robot dexterous manipulation," *IEEE Transactions on Haptics*, vol. 6, no. 2, pp. 129–144, 2013.

[2] Shadow Robot Company, "Shadow dexterous hand technical specification," https://www.shadowrobot.com/wp-content/uploads/shadow_dexterous_hand_technical_specification_E_20190221.pdf, accessed: 2019-08-16.

[3] S. W. Ruehl, C. Parlitz, G. Heppner, A. Hermann, A. Roennau, and R. Dillmann, "Experimental evaluation of the schunk 5-finger gripping hand for grasping tasks," in *2014 IEEE International Conference on Robotics and Biomimetics (ROBIO 2014)*. IEEE, 2014, pp. 2465–2470.

[4] H. Liu, K. Wu, P. Meusel, N. Seitz, G. Hirzinger, M. H. Jin, Y. W. Liu, S. W. Fan, T. Lan, and Z. P. Chen, "Multisensory Five-Finger Dexterous Hand: The DLR/HIT Hand II," in *2008 IEEE/RSJ International Conference on Intelligent Robots and Systems, IROS*, Nice, 2008, pp. 3692–3697.

[5] Schunk, "Sdh," https://schunk.com/de_en/gripping-systems/series/sdh/, accessed: 2019-08-16.

[6] C.-M. Chang, L. Gerez, N. Elangovan, A. Zisimatos, and M. Liarokapis, "On Alternative Uses of Structural Compliance for the Development of Adaptive Robot Grippers and Hands," *Frontiers in Neurorobotics*, vol. 13, p. 91, 2019.

[7] B. Calli, A. Walsman, A. Singh, S. Srinivasa, P. Abbeel, and A. M. Dollar, "Benchmarking in Manipulation Research: Using the Yale-CMU-Berkeley Object and Model Set," *IEEE Robotics and Automation Magazine*, vol. 22, no. 3, pp. 36–52, 2015.

[8] B. Sundaralingam and T. Hermans, "Relaxed-rigidity constraints: kinematic trajectory optimization and collision avoidance for in-grasp manipulation," *Autonomous Robots*, vol. 43, no. 2, pp. 469–483, 2019.

[9] N. Correll, K. E. Bekris, D. Berenson, O. Brock, A. Causo, K. Hauser, K. Okada, A. Rodriguez, J. M. Romano, and P. R. Wurman, "Analysis and observations from the first amazon picking challenge," *IEEE Transactions on Automation Science and Engineering*, vol. 15, no. 1, pp. 172–188, 2018.

[10] J. Leitner, A. W. Tow, N. Sunderhauf, J. E. Dean, J. W. Durham, M. Cooper, M. Eich, C. Lehnert, R. Mangels, C. McCool, P. T. Kujala, L. Nicholson, T. Pham, J. Sergeant, L. Wu, F. Zhang, B. Upcroft, and P. Corke, "The ACRV picking benchmark: A robotic shelf picking benchmark to foster reproducible research," in *IEEE International Conference on Robotics and Automation*, Singapore, 2017, pp. 4705–4712.

[11] A. Altobelli, *Sensorized Object Approach*. Cham: Springer International Publishing, 2016, pp. 21–41. [Online]. Available: https://doi.org/10.1007/978-3-319-47087-0_3

[12] R. Kõiva, R. Haschke, and H. Ritter, "Development of an intelligent object for grasp and manipulation research," in *2011 15th International Conference on Advanced Robotics (ICAR)*, June 2011, pp. 204–210.

[13] M. A. Roa, R. Kõiva, and C. Castellini, "Experimental evaluation of human grasps using a sensorized object," in *2012 4th IEEE RAS EMBS International Conference on Biomedical Robotics and Biomechatronics (BioRob)*, June 2012, pp. 1662–1668.

[14] National Institute of Standards and Technology, "Grasping performance metrics and test methods," https://www.nist.gov/el/intelligent-systems-division-73500/robotic-grasping-and-manipulation-assembly/grasping, accessed: 2018-11-1.

[15] J. Falco, K. Van Wyk, S. Liu, and S. Carpin, "Grasping the Performance," *IEEE Robotics and Automation Magazine*, vol. 22, no. 4, pp. 125–136, 2015.

[16] A. Singh, J. Sha, K. S. Narayan, T. Achim, and P. Abbeel, "BigBIRD: A Large-Scale 3D Database of Object Instances," in *IEEE International Conference on Robotics and Automation*, no. 4, Hong Kong, 2014, pp. 509–516.

[17] A. Kasper, Z. Xue, and R. Dillmann, "The KIT object models database: An object model database for object recognition, localization and manipulation in service robotics," *International Journal of Robotics Research*, vol. 31, no. 8, pp. 927–934, 2012.

[18] C. Goldfeder, M. Ciocarlie, H. Dang, and P. K. Allen, "The Columbia Grasp Database," in *IEEE International Conference on Robotics and Automation*, Kobe, 2009, pp. 1710–1716.

[19] R. R. Ma and A. M. Dollar, "An underactuated hand for efficient finger-gaiting-based dexterous manipulation," in *2014 IEEE International Conference on Robotics and Biomimetics (ROBIO 2014)*. IEEE, 2014, pp. 2214–2219.

[20] R. R. Ma, J. T. Belter, and A. M. Dollar, "Hybrid deposition manufacturing: design strategies for multimaterial mechanisms via three-dimensional printing and material deposition," *Journal of Mechanisms and Robotics*, vol. 7, no. 2, p. 021002, 2015.

[21] S. Madgwick, "An efficient orientation filter for inertial and inertial/magnetic sensor arrays," *Report x-io and University of Bristol (UK)*, vol. 25, pp. 113–118, 2010.

[22] M. Windolf, N. Götzen, and M. Morlock, "Systematic accuracy and precision analysis of video motion capturing systems—exemplified on the vicon-460 system," *Journal of Biomechanics*, vol. 41, no. 12, pp. 2776 – 2780, 2008. [Online]. Available: http://www.sciencedirect.com/science/article/pii/S0021929008003229

[23] "Liberty user manual 240/16," Polhemus, August 2012, Rev. H.

[24] S. Garrido-Jurado, R. Muñoz-Salinas, F. Madrid-Cuevas, and M. Marín-Jiménez, "Automatic generation and detection of highly reliable fiducial markers under occlusion," *Pattern Recognition*, vol. 47, no. 6, pp. 2280 – 2292, 2014.

[25] G. Gao, A. Dwivedi, N. Elangovan, Y. Cao, L. Young, and M. Liarokapis, "The new dexterity adaptive, humanlike robot hand," in *IEEE International Conference on Robotics and Automation*, 2019.

[26] R. Ma and A. Dollar, "Yale OpenHand Project: Optimizing Open-Source Hand Designs for Ease of Fabrication and Adoption," *IEEE Robotics and Automation Magazine*, vol. 24, no. 1, pp. 32–40, 2017.